NORTH-SOUTH ASYMMETRY IN MARTIAN CRATER SLOPES. R. A. Parsons[1], F. Nimmo[1] and M. D. Ellehoj, [1]University of California, 1156 High St., Santa Cruz, CA 95060 (rparsons@pmc.ucsc.edu)

Introduction: A significant amount of data suggests that water ice is present in variable concentration within the Martian shallow subsurface [1], [2]. Equatorial regions appear to be depleted in ice, while an ice mantle extends poleward of 30° [3]. Global roughness measurements suggest topographic relaxation at short wavelengths in mid-latitudes, possibly due to creep of ice-rich regolith [4]; this creep may also be responsible for the observed north-south asymmetry in slopes [5]. Relaxation of a deformable, presumably ice-rich, regolith layer of approximately 1 km in thickness may explain softened craters at mid to high latitudes [6]. Softened craters are characterized by rounding of the crater rims and by crater slopes that are more convex. Crater softening due to ice-driven creep may vary spatially within a single crater due to temperature variations induced by the angle of insolation. Because creep processes are more rapid at higher temperature, one would expect equator-facing crater slopes to be shallower than pole-facing slopes for low obliquities. In this study we focus on the current obliquity state of Mars in this study – generally applicable to the last 5 Myrs of Martian history. To test the crater slope asymmetry hypothesis, we measured crater slopes in the equatorial and north and south mid-latitude regions of Mars.

Theory: We quantified the effect of ice-rich soil creep on crater slopes using a simple one dimensional model. The relaxation of topography (*h*) is governed by the thickness, δ, of the ice-rich layer, the surface viscosity (η_{sfc}) of the creeping layer, and the local slope as shown in the following equation:

$$\frac{\partial h}{\partial t} = 2\delta^3 \rho g \frac{\partial}{\partial x}\left(\frac{1}{\eta_{sfc}}\frac{\partial h}{\partial x}\right) \qquad (1)$$

where ρ is the density of the creeping layer and *g* is gravity. The thickness of the ice-rich layer is defined as the depth at which the viscosity as increased by a factor of *e*. The viscosity at the surface of the creeping layer is given by (modified from [7])

$$\eta_{sfc} = \eta_o e^{\frac{Q}{RT} + b\phi} \qquad (2)$$

where *Q* is the activation energy, *R* is the ideal gas constant, *T* is the local temperature, ϕ is the dust fraction, and *b* is a constant. Both the latitude and the local slope are needed to determine the local temperature. The temperature of a horizontal surface on Mars is assumed to vary linearly with respect to latitude ranging from 220 K at the equator to 160 K at the poles. The local slope modifies this latitudinal varying temperature by ΔT where

$$\Delta T = T_\gamma \left[1 - \left(\frac{\cos(\gamma - \theta)}{\cos\gamma}\right)^{1/4}\right]. \qquad (3)$$

In equation 3, γ is latitude and θ is the slope angle. Using equations 1-3 we are able to soften an initial crater profile over time using specified values for latitude, δ, and ϕ. An example of a modeled topographic profile is shown in figure 1 for a 20 km diameter crater at 30° latitude with δ = 1000 m over a 5 Myr period.

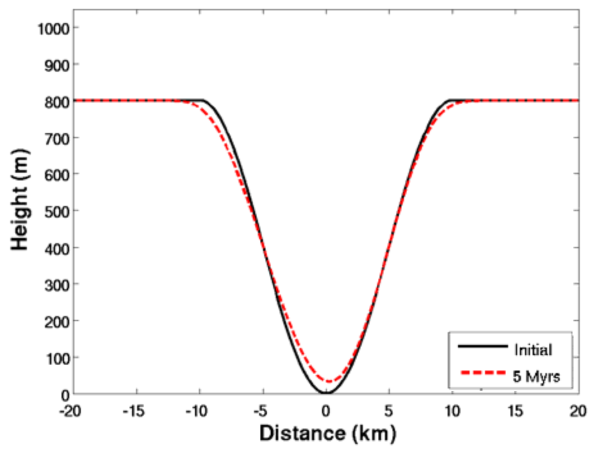

Figure 1. Simulation of 5 Myrs of topographic relaxation of a 20 km diameter crater at 30° latitude assuming a deformable layer 1000 m in thickness with a 10% dust fraction.

Notice the pronounced asymmetry in slope that has developed in the final profile due to the hastening of creep on the equator-facing slope (right hand side of crater). To quantify the slope asymmetry we defined the parameter *A* where

$$A = \frac{S_n - S_s}{S_{ave}}. \qquad (4)$$

S_n and S_s are the maximum slopes on the north and south faces, respectively and S_{ave} is the average maximum slope for the two faces. A negative value for *A* indicates that the south face of the crater is steeper in slope than the north face. In the next section, we use the average maximum slopes from the east and west crater faces to calculate S_{ave} using MOLA data. As a reference, the value of *A* in figure 1 is 0.27.

We derived an analytical solution to equation 1 by assuming a constant viscosity difference, between the north and south crater faces. We then determined how slope asymmetry would vary as a function of latitude, as shown in figure 2.

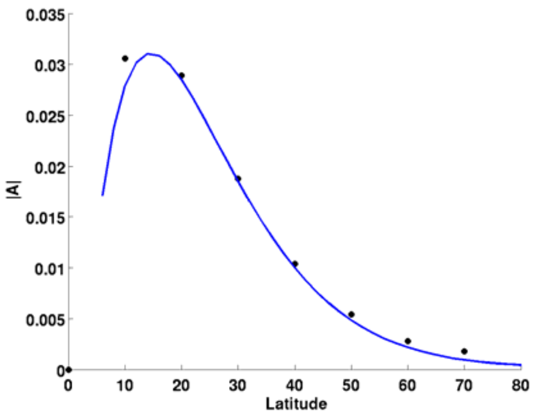

Figure 2. Analytical estimate (blue line) and numerical results (black dots) of the crater asymmetry parameter (*A*) as a function of latitude. These data assume a 20 km diameter crater and 1000 m thick deformable layer with a 10% dust fraction.

The blue line indicates the analytical solution to equation 1 using the aforementioned assumption whereas the black dots show the results from the full numerical solution. We conclude that the simplified analytical solution is satisfactory in representing how slope asymmetry varies as a function of latitude. The shape of the curve in figure 2 tells us that the temperature at the poles is too cold for flow to occur on either the equator-facing or the pole-facing slope, thus, no asymmetry develops. At mid to low latitudes the regional temperature is high relative to the poles. Also, ΔT is significant due the differences in incident sunlight between the north and south crater faces. This results in the local maximum in asymmetry at 15^{o} latitude. Finally, near the equator, the angle of incident sunlight is approximately the same for the north and south crater faces so no asymmetry can develop. Next we look for observational evidence of crater asymmetry at various locations on Mars.

Method: We analyzed relatively fresh craters ranging from 5 to 20 km in radius located in the mid-latitude northern (~30^{o}N), equatorial (~0^{o}), and mid-latitude southern (~30^{o}S and ~20^{o}S) regions of Mars. Radial topographic profiles were taken every 20 degrees, each extending from the center of the crater to just beyond the rim (dotted lines in Figure 3).

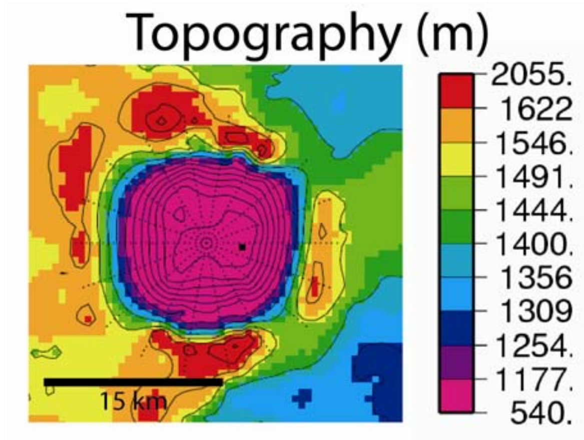

Figure 3. MOLA topography of a 16 km diameter crater at 1.5^{o}S, 33.2^{o}E. Topographic contours are made every 100 m. Dotted lines indicate locations of radial profiles used to measure slope.

A total of 18 profiles were made: 4 profiles transect the north and south crater faces and 5 profiles transect the east and west faces. The topography was sampled at a resolution of 375 m for all profiles. Next, we find the maximum slope for each profile and average the maximum slopes of the appropriate profiles together to get a value for the slope of a particular crater face. Finally, the crater slope asymmetry is quantified by the parameter *A*, where $A = (S_n - S_s)/S_{ew}$. In this expression S_{ew} is the averaged slope of the east and west faces.

Results: The observed crater slope asymmetry measured using topography is compared with the theoretical solution in figure 4. The colored dots are measured slope asymmetries for individual craters and the black squares indicate the mean value for a particular latitude region. As shown in this figure, there is no statistically significant slope asymmetry at any of the latitude regions we analyzed. This provides us with an upper limit on the thickness of the creeping ice-rich layer. The black lines in figure 4 show the expected asymmetry signal for a 30 km diameter crater evolving over a 5 Myr period for various creeping layer thicknesses. We conclude that the creeping layer is likely to be less than 1000 m thick; otherwise we would expect to see a more pronounced signal in the data.

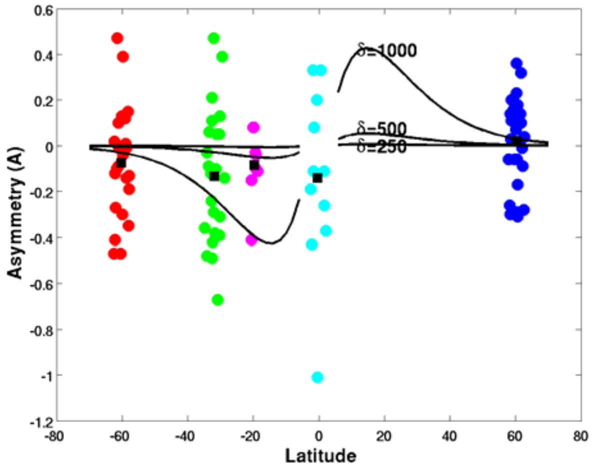

Figure 4. Observed crater asymmetry measured at various latitudes (colored dots) compared to theoretical results (black lines) for varying creeping layer thicknesses (δ) over a 5 Myr period. The black squares indicate the mean asymmetry values for a particular latitude region.

Conclusions: These analyses of crater slope asymmetry suggest a creeping layer thickness of less than 1 km – perhaps ranging from 500 m near the equator to 1 km near the poles. If there was a creeping layer 1 km in thickness or greater at low latitudes, we would expect to see a more pronounced asymmetry signal. However, there are a couple of alternative reasons why little asymmetry is observed in the topography. First, prior obliquity cycles may have caused craters to become asymmetric in the opposite sense than what we would expect to see today. Crater modification studies by Kreslavsky and Head, 2006 [8] suggest moderately high obliquity periods were probable during the last 40-160 Myr. The accentuated softening on poleward facing slopes during these periods of high obliquity would erase the asymmetry that would develop during a subsequent, low obliquity period. The strong dependence of crater softening on wavelength [6], [7] may be an alternative explanation of why no crater asymmetries are observed. Because short wavelength features will relax more quickly than longer wavelengths, it is possible that we much look at higher resolution topography to resolve crater slope asymmetry.

References: [1] Boynton W. V. et al., (2002) *Science, 297,* 81–85. [2] Feldman W. C. et al. (2002) *Science, 297,* 75-78. [3] Mustard J. F. et al. (2001) *Nature, 412,* 411-414. [4] Kreslavsky M. A. and J. W. Head, (2000) *JGR, 105,* 26695-26711. [5] Kreslavsky M. A. and J. W. Head, (2003) *GRL, 30,* 1815. [6] Jankowski D. G. and Squyres S. W., (1992) *Icarus, 100*, 26-39. [7] Pathare A. V. et al., (2005) *Icarus, 174,* 396-418. [8] Kreslavsky M. A. and J.W. Head, (2006) *Meteoritics & Planet. Sci., 41,* 1633-1646.